Random Copolymer inverse design system orienting on Accurate discovering of Antimicrobial peptide-mimetic copolymers

Tianyu Wu, Yang Tang, *Senior Member, IEEE*

Abstract—Antimicrobial resistance is one of the biggest health problem, especially in the current period of COVID-19 pandemic. Due to the unique membrane-destruction bactericidal mechanism, antimicrobial peptide-mimetic copolymers are paid more attention and it is urgent to find more potential candidates with broad-spectrum antibacterial efficacy and low toxicity. Artificial intelligence has shown significant performance on small molecule or biotech drugs, however, the higher-dimension of polymer space and the limited experimental data restrict the application of existing methods on copolymer design. Herein, we develop a universal random copolymer inverse design system via multi-model copolymer representation learning, knowledge distillation and reinforcement learning. Our system realize a high-precision antimicrobial activity prediction with few-shot data by extracting various chemical information from multi-modal copolymer representations. By pre-training a scaffold-decorator generative model via knowledge distillation, copolymer space are greatly contracted to the near space of existing data for exploration. Thus, our reinforcement learning algorithm can be adaptive for customized generation on specific scaffolds and requirements on property or structures. We apply our system on collected antimicrobial peptide-mimetic copolymers data, and we discover candidate copolymers with desired properties.

1 Main

In the current period of the continuous COVID-19 pandemic, antibiotics are intensively used and therefore the public health problem of antimicrobial resistance (AMR) is getting aggravated day by day [1], [2]. To overcome this issue, naturally occurring host-defense antimicrobial peptides (AMPs) have been widely researched as the next-generation therapeutics for AMR, benefited for the specific membrane-destruction bactericidal mechanism of AMPs [3]. However, difficulties of the over-costing and time-consuming production of AMPs which limit their large-scale production [4]. Antimicrobial peptide-mimetic copolymers, which mimic the cationic-hydrophobic amphiphilic structure of AMPs with the bactericidal mechanism, have been paid more attention in recent years. These copolymers has the advantages of low cost, easy synthesis and high structural flexibility, thus scientists are devoting to finding new copolymers with broad-spectrum antibacterial efficacy (e.g. S.aureus and E.coli) and low toxicity as therapeutic drugs (Fig 1(a-b)) [5].

Benefiting from the integrated big data, artificial intelligence (AI) has shown significant performance on revealing the implicit bioinformatics and exploring the large-scale chemical [6], [7], [8], [9], [10]. Compared with traditional drug design pipeline of high-throughout experiments or empirical design, AI design has been proved to greatly accelerate the whole process of drug discovery with high efficiency [11], [12], [13]. Similarly, in virtue of the AI techniques, we use the existed antimicrobial data to design new candidate antimicrobial peptide-mimetic copolymers as potential drugs (Fig 1c).

For antimicrobial peptides design, most proposed methods are mainly objected to sequence-defined situation, focusing on designing the arrangements and the quantities of various motifs [12], [14], [15]. However, most peptide-mimetic copolymers are random copolymers with clear component information and unknown sequence order, which means methods for peptides are difficult to be transferred for further usage.

As random copolymer, the principal factors which influence the antimicrobial activity are the structures of each polymerized monomers and the composition between them. In this way, we conclude the two following problem to concern inspired by the idea of inverse design [16] : 1) how to accurately predict the properties of random copolymer from limted experimental data, e.g. the antimicrobial activity on various strains and the toxicity, with deterministic monomer structures with corresponding ration information, 2) potential drug-like small molecules was estimated to be between 10^{30} and 10^{60} [17], and for binary copolymers, the number would be boosted to an inestimable degree, thus how to explore the vast combinatorial space is a challenging problem.

In this study, we fully consider the concerns above and we design a universal random copolymer inverse design framework, including prediction and generation, which can be transferred to other scenarios with high efficiency and flexibility. For random copolymer predictor, previous works have proposed several strategies for the property prediction of random copolymers [18], [19], [20]. The common ground of these methods is that only one single copolymer representation, involving Morgan Fingerprints, graph embedding or molecular descriptors is chosen. A constellation of researches have proved the effectiveness of fusing multiple molecular representations for predicting the properties of small molecules with extracting more comprehensive information [21], [22], [23]. Inspired by this, we firstly propose three different copolymer representations embedded with

important chemical information for prediction for further fusion.

In particular, we introduce a machine-learning based method for the optimal molecular descriptors downselection for specific tasks [24] and we refer to BigSMIES syntax [25] to construct polymeric sequence representation and graph representation (See Methods). Thus, we develop a polymeric feature representations fusion strategy with considering the relevance and dissimilitude between different representations. By combing multiple representations, we construct accurate quantitative structure–property relationship (QSPR) models even if the datapoints are limited.

For random copolymer generator, we develop a reinforcement learning (RL) based monomer scaffold-decorator model via knowledge distillation. With given specific scaffold structures, the RL agent learn molecule grammar and generate thousands of monomer structures in the learning process. Through further designing multiple constrains as proper reward functions, the model can generate molecules with desired properties.

In this study, we use our framework on the design of antimicrobial peptide-mimetic copolymers. With AI, we design and filter for new copolymer structures and we further prove the effectiveness of generated copolymers through synthetic experiments.

We collect the data of cationic-hydrophobic amphiphilic β-amino acid polymers (Fig 1d) from previous literature to formulate the random copolymer dataset [26], [27], [28], [29]. β-amino acid polymers are a kind of bipolymer with changeable cationic and hydrophobic side chains as R1, R2.

We aim to adjust the structure of R1 or R2 to find more potential candidate copolymers which have desired properties of S.aureus< 25, E.coli< 25, HC10> 100. We collect totally 86 existing datapoints, while generally it is hard to find a satisfying balance between antimicrobial activity and toxicity (Fig 1e).

With this AI system, we have efficiently discovered superior performance of highly selective broad-spectrum antibacterial compounds based on existing low selective anti-positive and anti-negative copolymers through synthesis validation.

2 Results

Overview of antibacterial drug discovery. In this study, we target to discover candidate ationic-hydrophobic amphiphilic β-amino acid polymers with highly selective broad-spectrum for the usage of antibacterial drug though aritificial intelligence. Main procedures include data process, property prediction and polymer generation (Fig 2). We collect a library of polymers with different racemic cationic and hydrophobic subunits, involving DM ("dimethyl"), MM ("monomethyl"), CP ("cyclopentyl"), CH ("cyclohexyl"), etc (Fig 2a). Totally 86 datapoints are collected with different cationic and hydrophobic subunit composition on three desired properties (MIC value of S.aureus and E.coli, and the value of HC10). Considering the permutation invariance [19] in multicomponent systems with randomly assocaited components, such as random copolymers, we apply a simple data augmentation method with considering the permutation invariance (Fig 2b), and we enlarge the amount data from 86 to 172 (See Methods).

For each copolymer, we design three ways for random copolymer featurization from the respective of molecular descriptors and molecular representations (Fig 2c). With Morded calculator [30], near 4000 descriptors are calculated and we apply a machine learning based downselection [24] (See Methods). Then, feature vectors of cationic and hydrophobic subunit are stacked to represent a random copolymer. We further refer to BigSMILES syntax [25] which has been nearly proposed in polymer informatics. According to the syntax, we design a sequence representation with embedding ration information and bonding descriptors to represent a random copolymer. Analogously, we introduce the linking rules of bonding descriptors as new nodes and edges in graph representation. Noted that both sequence and graph are direct representations for the monomer topology with rich latent relative information embedded (See Methods).

All the feature vectors would be sent to the predictive network to train the QSAR model which quantify the needed properties (MIC value of S.aureus and E.coli, and the value of HC10) of the input random copolymer. Thus, we develop a polymeric feature representations fusion strategy with considering the relevance and dissimilitude between different representations (Fig 2d). We apply a FNN, a GRU [31] and a GNN [32] for feature, sequence and graph representations respectively to extract the embedded chemical information, and we adjust different network architectures (Supplementary information) to find the optimal input combination. We use a transformer-based framework [33], [34] which aims at extracting feature correlations and differences between molecular descriptors and molecular representations by adding an attention bias.

With accurately predicting the MIC value of S.aureus and E.coli, and the value of HC10, through knowledge distillation we pretrain a scaffold-decorator model for different targeted scaffolds (Supplementary Figure 1) with polyamide backbone similar to natural peptides. Technical details can be found in Methods. Then, we use reinforcement learning (RL) to fine-tune the pretrained decorator model to generate copolymers with desired properties step-by-step (Fig 2e). The predictive model and the pretrained decorator model are seen as the environment and the agent in RL settings. And the values calculated by the predictive model would be transform as rewards to adjust the direction for next molecule sampling. With iteration, we filtered out the candidate copolymers for antibacterial experiments.

Performance on Feature selection. First, we make experiments to prove the effectiveness of applying data augmentation and feature optimization, since these are two important operations which may influence the data or feature input for training. We define D1 and D2 as the original data and the augmented data. We chose 20% of the D1 and D2 as the unseen set, and we construct RF (Random Forest) models trained by the rest 80% of data for comparison on various features (See Methods). We make a 20-fold cross validation with calculating the metric of R2 (higher the better) on predicting MIC of S.aureus and HC10, and results are shown in Fig 3a. (More in supplementary information). The results show that with applying data augmentation, it brings a 20.3% mean increase and a 6.7% mean increase for predicting MIC of S.aureus and HC10 on different features,

respectively. With applying feature optimization, it brings a 26.3% mean increase of R2 for each situation. These results prove the necessity of applying these two operations, and the data augmented and the feature optimized would be used for further learning.

Performance on Fusing strategies. Then we evaluate the predictive performance on different fusing strategies of various copolymer representations. In this study, we try five combinations including 1) SMILES only, 2) Feature only, 3) Feature and Graph, 4) Feature and SMILES, 5) Feature and SMILES and Graphs. Similarly, the data and the experimental settings are the same with the last part. We evaluate the mean R2 (higher the better) and the RMSE (lower the better) scores of predicting MIC value of S.aureus and the value of HC10 on the unseen set of D2. As Fig 3b. shows, the combination of Feature and SMILES surpasses the others. We further evaluate the predictive performance of the trained model on all data in D2 , shown in Fig 3c. Also, "Feature and SMILES" show the best performance and both of the R2 metrics reach the value of 0.9. We further visualize the predicted results with the measured results in Fig 3d with the final model, which shows that our predictive model shows high accuracy the antimicrobial activity prediction even with limited data.

Monomer generation on various amino acid scaffolds. In our architecture, predictive network leads the directions of generative model when exploring the chemical space in the process of copolymer inverse design. To find more hidden possible cationic-hydrophobic amphiphilic β-amino acid polymers, our target is to optimize or search for new side chain structures with keeping the main chain intact. Tradition molecular generative pattern generally focus on creating molecules character-by-character from scratch [6], [35], [36] which is unfit for customlized structural constraints on scaffolds. In this way, we propose a reinforcement learning based molecular scaffold decorator generative model [37] via knowledge distillation for new copolymer design. Details are shown in Methods.

By running our model on different scaffold structures with constrains of carbon number (in range of 11) and ring number (in range of 1), we collect 1840 monomer structures with all passing the drug-likeness rules (See Methods) and we make easy statistic analysis on them, shown in Fig 4a. All scaffolds involved are shown in Supplementary information. From Fig 4a, it can be clearly found that scaffold 1-3 have more monomer structures, while for scaffold 4-6 the monomer structures have a obviously decrease. It is a reasonable phenomenon since ring structures have fixed structure and carbon number, and the space for adjustment on scaffold 4-6 is much smaller. Noted that, results here mainly prove that our model can adaptive to generate monomers on various amino acid scaffolds. Noted that, these numbers are not accurate since we pay put more attention on the partial scaffolds.

Property Distribution combing with DM and MM cationic monomers We make predictions on the MIC value of S.aureus and E.coli, and the value of HC10 with different ratio combination between the cationic monomer of DM or MM and the hydrophobic subunit generated. Thus, we visualize the three predicted property distribution and we separate different carbon numbers with different colors, shown in Fig 4b (DM as cationic monomer) and Fig 4c (MM as cationic monomer). It can be obviously found that copolymers in DM series have better mean antimicrobial activity on S.aureus and E.coli, while MM series seems to have a higher hemolysis which means a lower toxicity. Moreover, it can also be discovered the enormous influence which the carbon number brings. Generally, the more carbons the hydrophobic side chain monomer haves, the higher predicted antimicrobial activity and lower predicted hemolysis the copolymer may reach.

Visualization. To visualize the distribution of the generated monomer structures, we use uniform manifold approximation and projection (UMAP) [38] to project all molecules into 2D embedding in different chemical space, shown in Supplementary information. Results show that copolymers with similar property are generally clustered together.

To further filter out the candidate copolymers combing with DM structure, we visualize the chemical space with selection index (SI), which is used to judge the safe range of drug effect. We calculate the SI values on S.aureus and E.coli of all generated copolymers, and we classify them according to the range of SI, shown in Fig 5. By given specific cationic/hydrophobic ration, we generate 9 desirable candidate copolymers (both SI$>$10), including 4 different monomers. These copolymers are clustered near in UMAP space, and thus we assume that more hidden candidate copolymers can be found in their near space. With further considering the synthesis complexity of these structures, we decide to make deep exploration on the monomer A, calling BU-like series due to the structure similarity. choose the monomer A, which is similar to BU, for further research.

Generation Distribution on BU-like series As discussed, we focus on generating more monomer structures of BU-like series, which have only one linear chain structure. We run reinforcement learning on scaffold 1 with adding ring penalties and carbon number constrains, thus the model would generate more single chain structure. In supplementary information all structures generated are shown and we project them in 3D-space with the three properties as coordinate, shown in Fig 6a. Given the space limitations, we pick out several monomers with gradually increasing carbon number shown in Fig 6b. Properties and SI of these monomers with different ration composition of DM are displayed, and as expected these copolymers have desirable properties when fitting to an appropriate ration.

3 Discussion

In this study, we develop a universal random copolymer inverse design system via multi-model copolymer representation learning, knowledge distillation and reinforcement learning. Compared with traditional copolymer design pipeline, our model can rapidly and accurately locate to potential copolymers with desired properties with applying artificial intelligence techniques. With utilizing different information in multi-modal copolymer representation, our model achieves outstanding performance on adaptively predicting copolymer properties with limit data. On the basis of constructing high accurate predictive model, we train a scaffold-decorator model based on knowledge distillation and reinforcement learning. With given specic scaffold

structures, our model explore thousands of new monomer strucutures under the inverse design pattern. Moreover, our model is adaptive to multiple customized constrains, including properties or structures. Since both of our predictive model and generative show great adaptability for few-shot samples, our model is friendly to real-world application.

4 METHODS

4.1 Dataset Formulation

Polymer Data Collection. For the sake of exploring new structure for antimicrobial host defense peptides with the help of artificial intelligence, MIC value on S.aureus and E.coli, and HC10 of cationic-hydrophobic amphiphilic β-amino acid polymers with tunable subunit ratio are collected, with the total number of 86. These data is all collected from previous literature [39], [40], [41], [42], [43] and involves 2 cationic and 9 hydrophobic side chains. If the end point of bacterial growth had not been arrived during the experiment, the values was estimated to be the current available value. (e.g., for the experimental estimated value HC10>400, it is seen as 400 ug/mL). Noted that log transformation is performed to all the estimated results due to the regular values so that all the results are transformed as integers for constructing QSAR models.

Copolymer Data Augmentation. An important property for cationic-hydrophobic amphiphilic β-amino acid polymers, or more specifically for binary copolymers is that the machine learning model used should follow the permutation invariance of copolymer input components [19]. Meaning that the results of the model should not be influenced by the order of the components, and it can be formulated as,

$$\begin{cases} H = M_1[(p1, r1), (p2, r2)] = M_1[(p2, r2), (p1, r1)], \\ S = M_2[(p1, r1), (p2, r2)] = M_2[(p2, r2), (p1, r1)], \\ E = M_3[(p1, r1), (p2, r2)] = M_3[(p2, r2), (p1, r1)], \end{cases} \tag{1}$$

where H, S, E are the MIC values of S.aureus and E.coli, and the value of HC10, respectivly, while p, r are the polymer unit. We exchange each ationic-hydrophobic pair to hydrophobic-ationic pair expression when encoding them, and thus our predictive model is capable of focusing on the information of the monomer structures and the ratio. In this way, we reasonably introducing this property as a method for data augmentation, aiming at improving the accuracy of the predictve model. Deatailed, we exchange the order of the input hydrophobic-cationic units, thus the order of both chemical descriptors and BigSmiles sequences is also changed with same property label. Both the origin data and the exchanged data are used for machine learning.

4.2 Random Copolymer Featurization

. Translating polymers into machine readable features is one important problem with ongoing concerns for polymer informatics [44]. Different from micromolecules with deterministic topology connections of atoms and bonds, it is hard to represent random copolymers with unregular sequence by general representation methods (e.g., SMILES or graphs) due to the intrinsically stochastic nature of polymers [25]. Generally considering, the property of a copolymer is mainly decided by 1) types of monomers and 2) monomer sequence distributions, while for random copolymers, monomer ratio should be further taken into consideration. In our work, we approach the random copolymer featurization problem from the following two perspectives.

Molecular descriptors fingerprints. Molecular descriptors are mathematical representation of chemicals which are generally used to build QSAR models. We use Mordred calculator [30], which includes 1826 two- and three-dimensional descriptors and can be used freely. For our cationic-hydrophobic polymers, descriptors of both the cationic and hydrophobic unit are calculated and stacked together, totally dimensioned 3654 for candidate descriptor vector as $Init.$ with adding ration information $r1$,$r2$ of two monomers.

Feature Optimization. Then we apply a two-stage feature optimization strategy with a stage of statistical downselection and a stage of machine-learning based downselection [24]. In first stage, constant or almost constant descriptors are dropped from the initial set (Init., 3654 descriptors), and descriptors with variance less than 10% of the mean value across the Init. set (Var., 1018 descriptors) are filtered out. Next, we evaluate Spearman rank correlations of each descriptor pair, and descriptors with correlation higher than 0.9 as well as correlation with the target property ($HC10, S.aureus, E.coli$) higher than 0.05 are filtered out as (Cor., 171 descriptors).

In the second stage, a recursive feature elimination (RFE) method [45] is introduced on the Cor. descriptors set based on random fronest (RF) model. With RF regression, each descriptor is eliminated recursively according to the importance rankings until the last descriptor. Then, a 20-fold cross-validation is adopted with repeated stratified subsampling descriptors. The principle of choosing the optimized descriptor set is that set results the lowest mean RMSE. In this way, descriptors with most important or most relative information on the target property are selected. In our work, we choose 40 (which is changeable) descriptors as the optimized molecular descriptors (Opt., 40 descriptors) for part of the input of the predictive network.

Molecular representation. Molecular representation is another popular way to encode molecules. In recent polymer informatics, BigSMILES is a recent developed structurally-based line notation to reflect the stochastic nature of polymer molecules [25]. Compared with molecular descriptors, hidden chemical information can be learned from molecular representation via the data-driven pattern. According to the syntax of BigSMILES, we derive two kinds of rules to define a cationic-hydrophobic amphiphilic β-amino acid polymer.

Sequence fingerprints. Traditional SMILES strings are generally consist of atom tokens(e.g.“C”, “O”,“[NH3+]”), bond tokens(e.g.“=”, “#”) branching tokens(e.g.“()”, “1,2”) to encode molecules. In BigSMILES sequence, the stochastic object and the bonding descriptors are two new joined elements compared with basic SMILES grammar. We further make several additional definition so as the ration information of each repeat unit in the stochastic object can be expressed. Take $DM_{50}CO_{50}$ as an example, it can be written as: {[>]NC(C)(C)C(C[NH3+])C=O.[+rn=50],

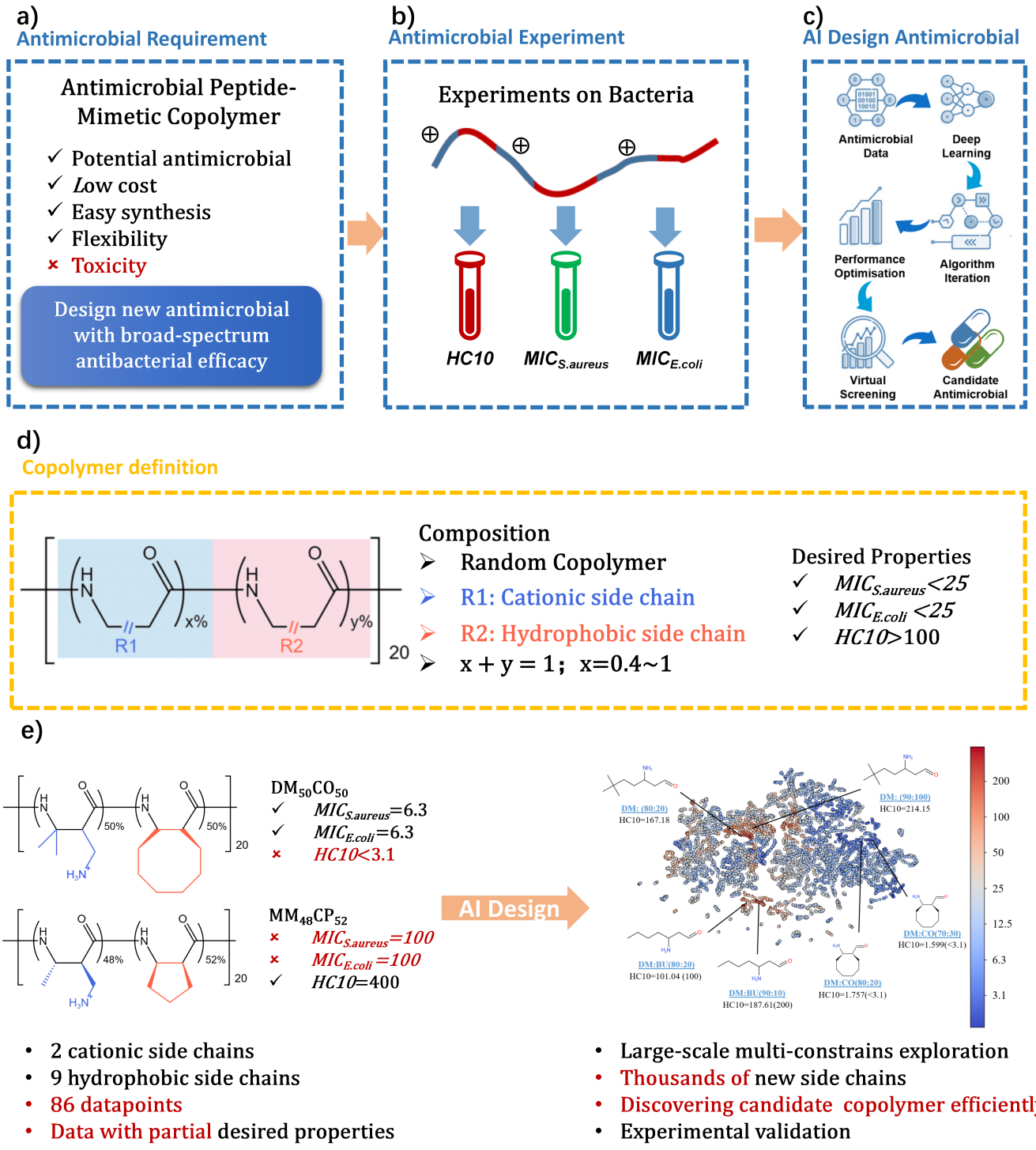

Fig. 1. **Motivation, definition and designation**. a) Highly challenging antimicrobial peptide-mimetic copolymer design requirements. b) Existing experimental antimicrobial dat collected from literature or laboratory experiments. c) General workflow of our artificial designation process with the collected data. d) Definition of the β-amino acid polymers with cationic and hydrophobic structures e) Through few positive data, various of monomer structures are generated and candidate copolymer are filtered our for experimental validation.

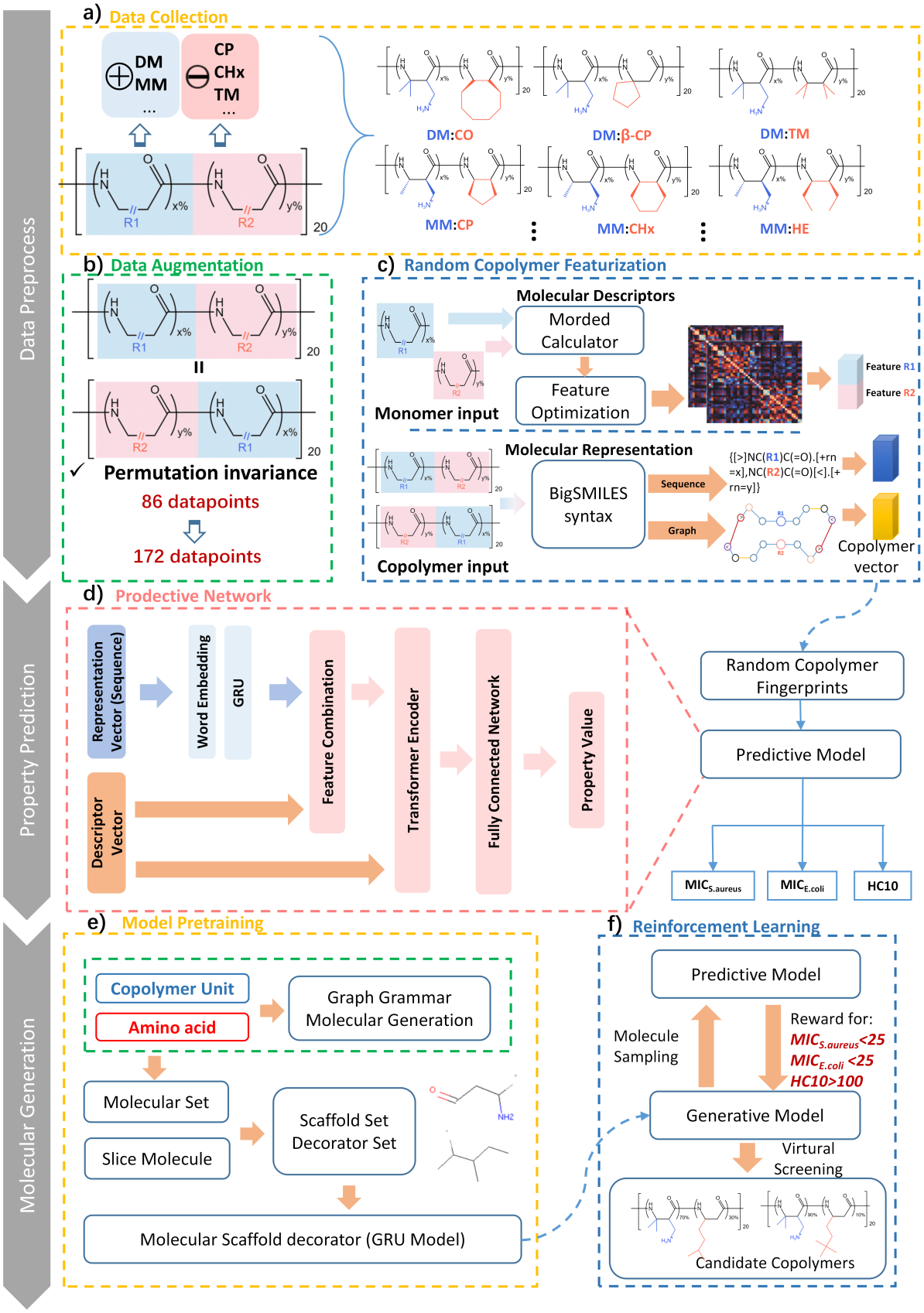

Fig. 2. **Workflow of antibacterial design.** a) Copolymer structures with tunable ationic-hydrophobic composition utilized in this work. b) Data augmentation method of permutation invariance for binary random polymers. c) Three ways for random copolymer featurizaztion. 1) Molecular descriptors of the cationic and hydrophobic monomers are calculated by the Morded calculator, number 3654. Through a feature optimization process, 40 descriptos are finally chosen as the copolymer feature vector. 2) Sequence representation defined by BigSMILES syntax, and monomers and ratio are shown as R1, R2, x and y. 3) Graph representation defined by BigSMILES syntax, and nodes or edges are defined by atoms (C, N, O) or bond (single or double). d) Network structure of combing molecular descriptors and the sequence representation which is used as predictive model in reinforcement learning. e) Process of pretraining the scaffold-decorator model which is used as the generative model in reinforcement learning f) Reinforcement learning diagram for candidate copolymer generation.

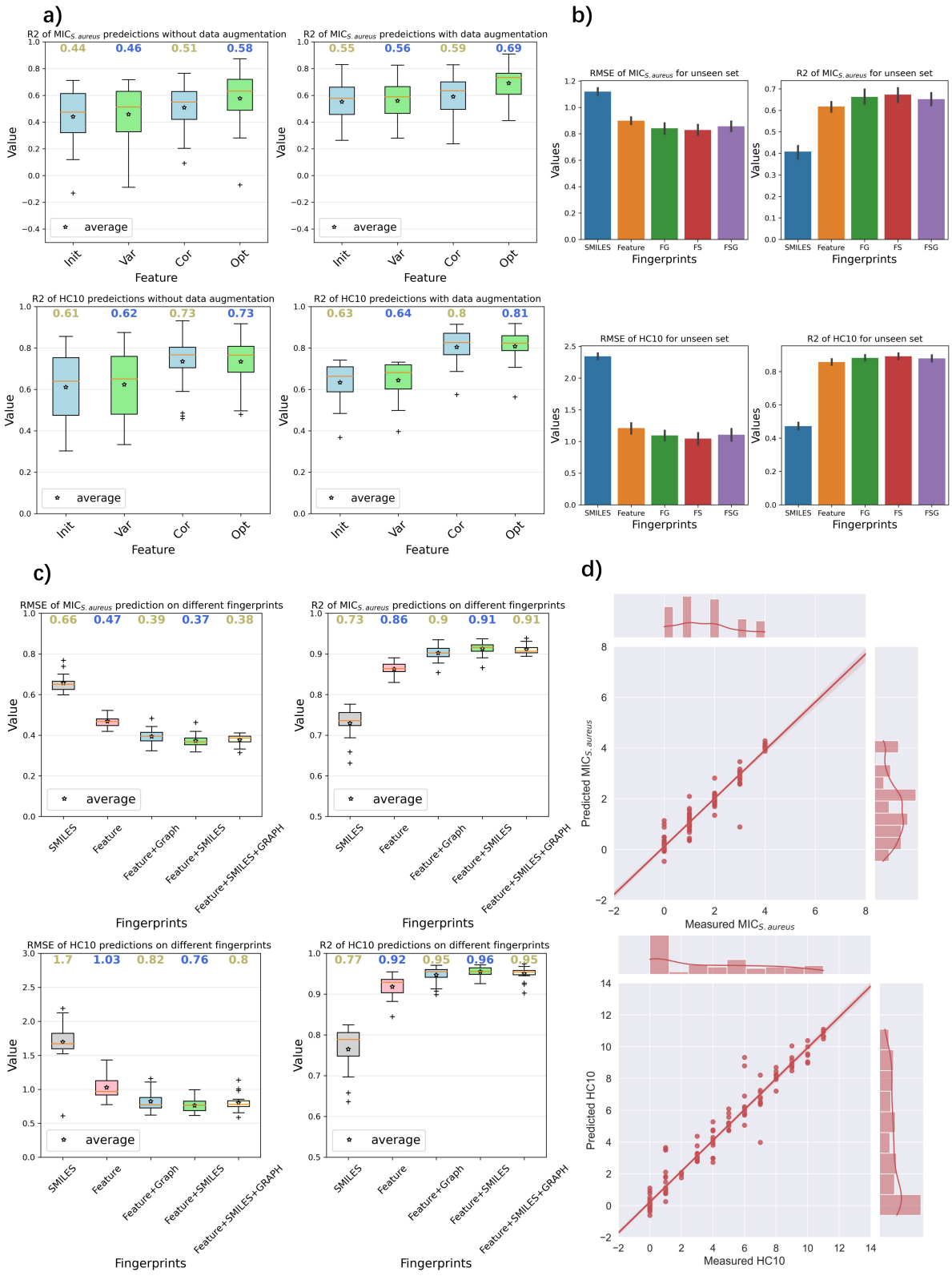

Fig. 3. Results on property prediction. a) Predictive results on MIC value of S.aureus and the value of HC10 on the unseen set of the data with and without augmentation on different feature selected. b) Predictive results on MIC value of S.aureus and the value of HC10 on the unseen set of the data augmented on different copolymer representation used in this work. c) Predictive results on all the data with different copolymer representations. d) Comparison between the predicted values and the measured values with the final model.

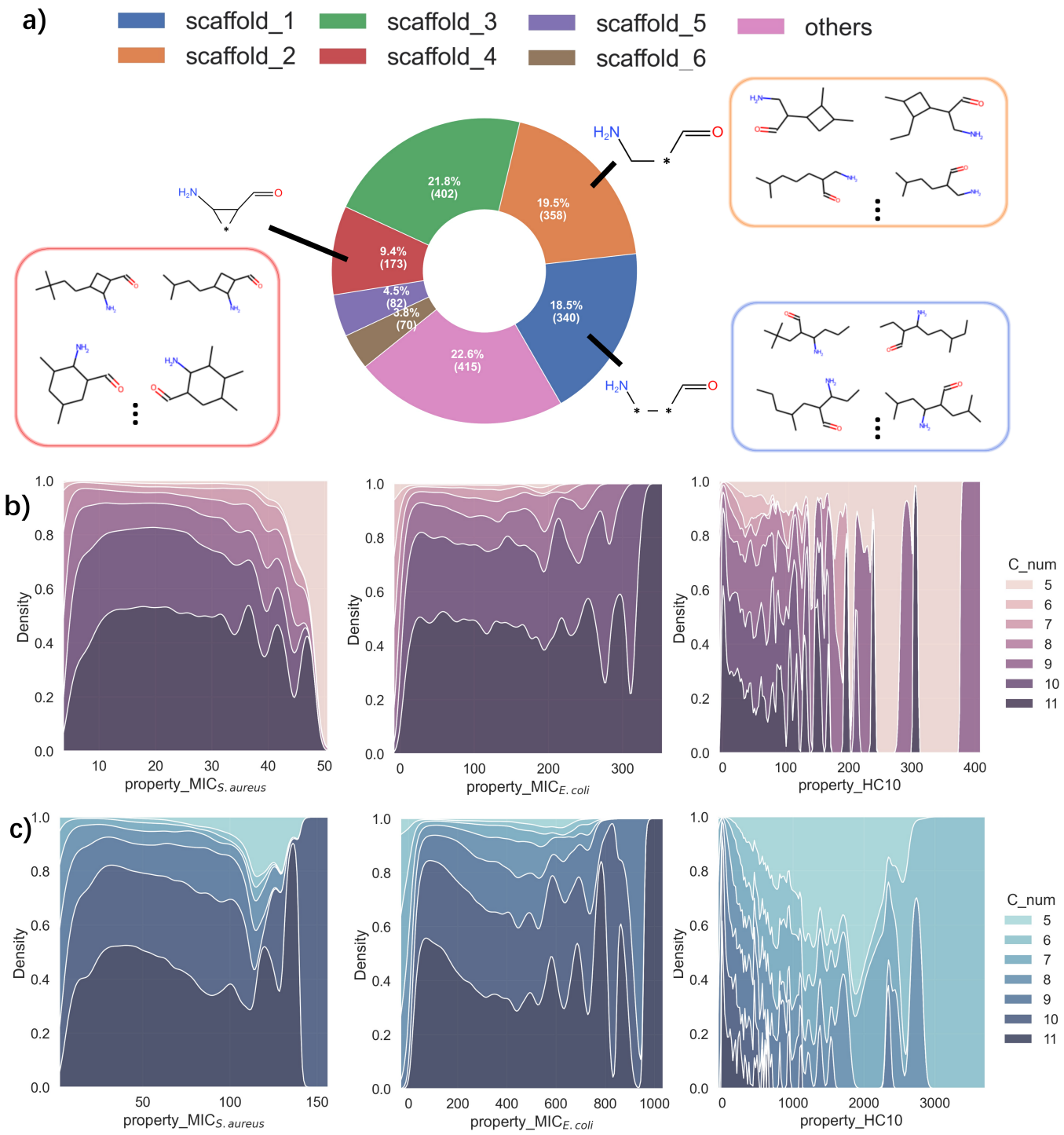

Fig. 4. Copolymer monomer distribution on scaffolds and different properties. a) Numbers of monomers generated by different scaffold structures. b) Property distribution on monomers combing with DM structures under carbon numbers of hydrophobic monomers ranging from 5 to 11. c) Property distribution on monomers combing with MM structures under carbon numbers of hydrophobic monomers ranging from 5 to 11.

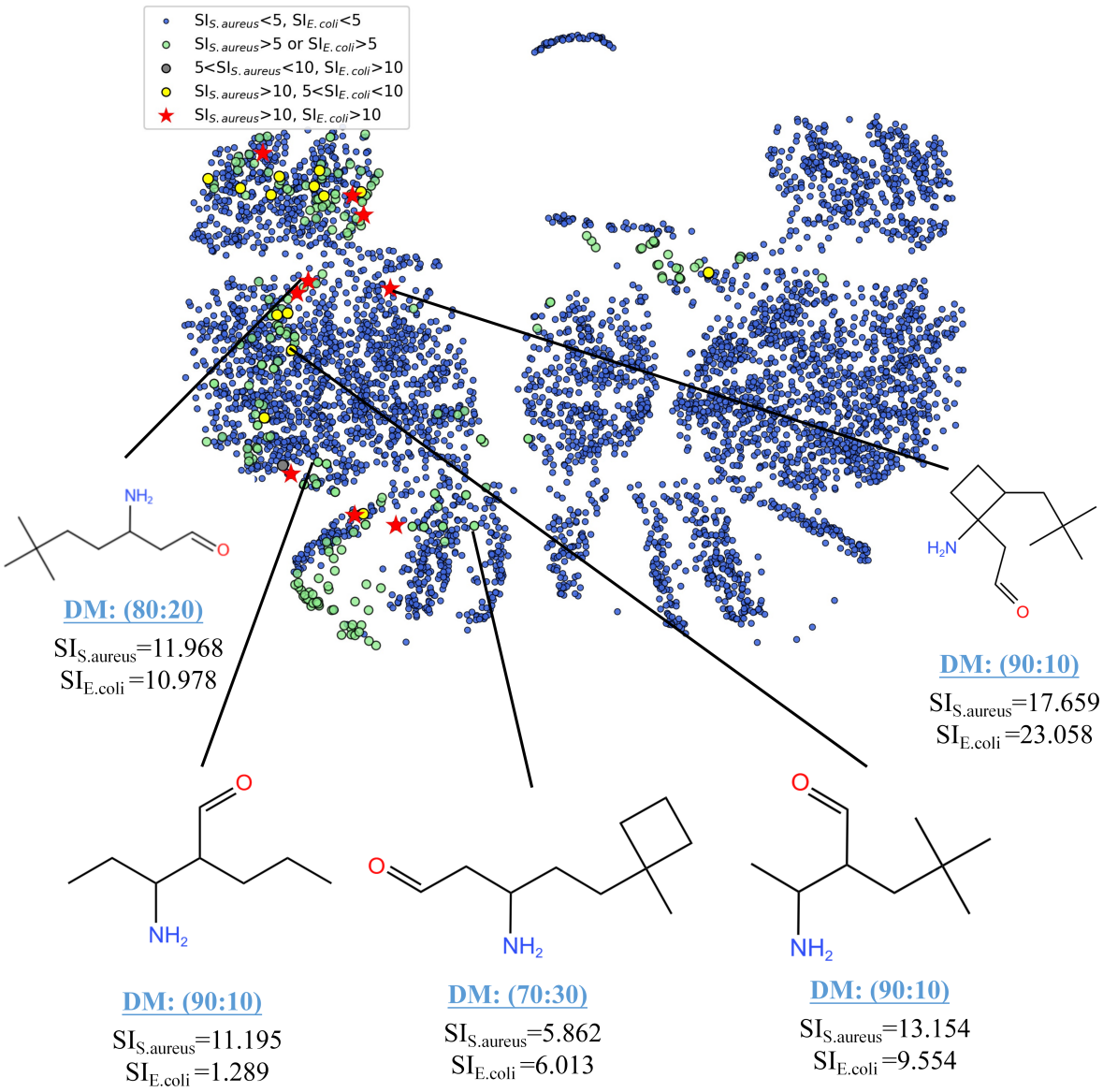

Fig. 5. Overview of the UMAP colored by the SI values on different strains. Each copolymer is colored according to the values of the calculated SI by the predictions on HC10, MIC of S.aureus and E.coli. Copolymer information with high SI are dispalyed.

NC1CCCCCC1C=O[<].[+rn=50]}, where [+rn=50] shows that DM unit has the ratio of 50%. ">" and "<" are two conjugate types of boding descriptors showing how repeat units are linked. For simplicity, we omit exterior strings and we use the simplification style. Other cationic-hydrophobic polymers are defined like such. After collecting all characters involved (shown in supplementary information), the one-hot encoding of the BigSMILES strings can be generated as the input.

Graph fingerprints. General used molecular graphs can not represent the stochastic nature of polymer molecules since graphs show clear topology structures of molecules. Inspired by BigSMILES syntax, we introduce new nodes and edges to define the bonding descriptors to take over traditional molecular graphs. Details can be seen in supplementary information. Noted that this kind of definition still exclude the ratio information of monomers and can be improved further.

4.3 Predictive network

We testify the performance on three target activity via different combination of fingerprint vectors: 1) Feature vector (molecular descriptors), 2) SMILES vector (BigSMILES sequence vector), 3) Feature vector and Graph vector (FG), 4) Feature vector and SMILES vector (FS), 5) Feature vector, SMILES vector and graph vector (FSG).

For situation 1), we simply train a Fully-connected Feed-forward Neural Network (FFN) with transforming the feature fingerprint F_f by subtracting the means and dividing by the standard deviations as normalization.

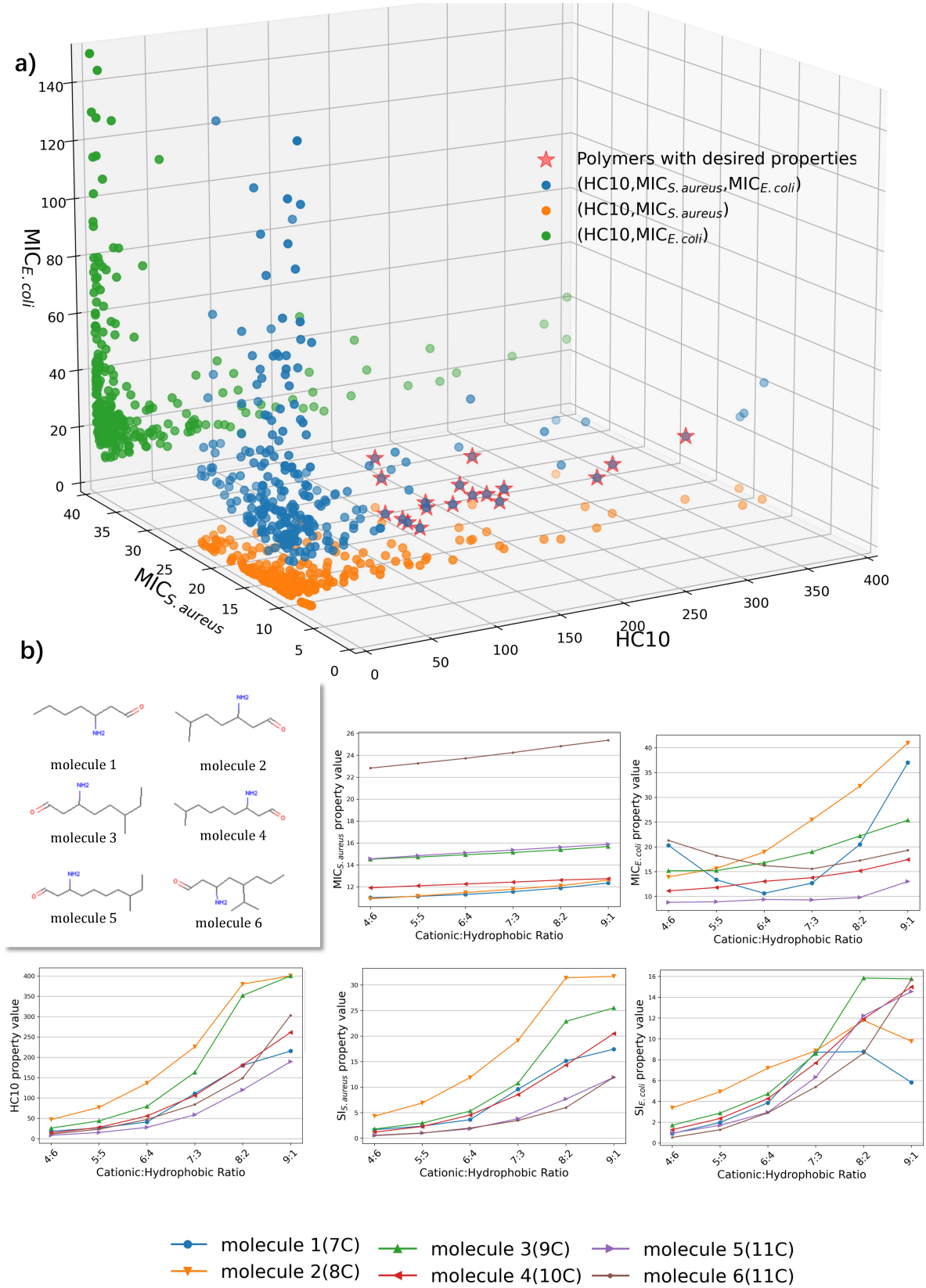

Fig. 6. Overview of the properties of BU-like series structures. a) 3D-projection of the generated BU-like series of three properties. Orange plots are the projection on (HC10, S.aureus) space, while green plots are the projection on (HC10, E.coli) space. Red stars are copolymers with desired properties of three. b) Properties of partial monomers structures under different ratio distribution and carbon numbers.

For 2), we use bidirectional Gate Recurrent Unit (GRU) to extract the hidden information embedded in BigSMILES sequence vector, and this progress can be formulated as,

$$\begin{cases} \overrightarrow{h_k} = \overrightarrow{\mathbf{GRU}}(t_k, \overrightarrow{h_{k-1}}), \\ \overleftarrow{h_k} = \overleftarrow{\mathbf{GRU}}(t_k, \overleftarrow{h_{k-1}}), \end{cases} \tag{2}$$

where t_k is the token embedding, and $\overrightarrow{h_k}, \overleftarrow{h_k}$ are bidirectional hidden states for the k th token of a BigSMILES string embedded by GRU, and the current hidden state h_k is obtained as,

$$h_k = (\overrightarrow{h_k}, \overleftarrow{h_k}). \tag{3}$$

Finally, we use F_s to denote the contextual representation of a BigSMILES string with length n as,

$$F_s = (h_0, h_1, \cdots, h_n). \tag{4}$$

Since 3), 4) and 5) involve multiple fingerprint vectors, we develop a multi-modal information learning framework with adiustable network blocks for specific fingerprints. A core motivation is how to learn more abundant chemical information from limited data points and how to find similarities and differences between information in diverse fingerprinting dimensions. From feature fingerprint, various basic chemical or calculated information can be gained. In contrast, from SMILES fingerprints or graph fingerprints, distributions of atoms and bonds on spatial and numerical are explicitly displayed, while more implicit information which may not be calculated through a specific equation is generally learned with the help of data-driven deep learning. Since available data is limited, to learn better copolymer feature for target prediction, we tempt to merge various fingerprints of which is one of the main contributions of our work.

The main structure includes several customized fingerprint learning blocks to extract implicit information from various fingerprints (Feature, SMILES and Graphs here), and this process can be formulated as,

$$\begin{cases} F_g = \mathbf{GNN}(G), \\ F_j = \mathbf{Combine}(F_f, F_s, F_g), \end{cases} \tag{5}$$

where G is the graph structure of copolymer and F_j is the joint feature by stacking all the features, and for graph fingerprints, Graph Neural Network (GNN) is introduced (details shown in supplementary information). According to the input fingerprints in 3), 4) and 5), different block is inserted. Noted that since fusing graph-based fingerprints does not reach desirable results after large amounts of experiments (shown in Fig and supplementary materials), which is mainly because ratio information is hard to be embedded in graphs. In this way, we finally give up adding graph fingerprints and details on the GNN used can be found in supplementary materials.

Then a Transformer-based feature combination block is built with the input of F_j after fingerprint fusion. Transformer has been proved as a powerful model on various fields through its power on extracting global information. To find the connections between different fingerprints (e.g. ratio information with different expressions), we further use feature descriptors F_f as the attention bias in the self-attention mechanism, and this process can be formulated as:

$$Q = F_j W_Q, K = F_j W_K, V = F_j W_V \tag{6}$$

$$\mathbf{Attention}(F_j) = \mathbf{softmax}(QK^\top/\sqrt{d_K} + F_f)V, \tag{7}$$

where W_Q, W_K, W_V are corresponding projecting matrices of Q (query),K (keys),V (values), and d_K is the dimension of keys. We use the Mean Squared Error (MSE) loss to train the model, and details of the hyperparameters of each block and the training protocols can be found in supplementary materials.

4.4 Generative network

Scaffold decorator. Take the hydrophobic monomer as an example, its SMILES representation is "NC(CCCC)CC=O", which can also be seen as that a side chain "[*]CCCC" is decorated to the scaffold "NC([*])CC=O", where "[*] is the special attachment token". For scaffold with more than one attachments, a symbol "|" is introduced to differentiate decorations. Therefore, the core problem of copolymer design can be transformed as finding the optimized decoration for the specific scaffold to formulate the part or both of cationic or hydrophobic monomer in copolymer with desirable properties. We summarize the whole designing procedure as two stages. Firstly, we pretrain a GRU-based molecular scaffold-decorator with the ability of generating valid molecules. Secondly, a reinforcement learning fine-tuned stage is adopted to explore the chemical space for candidate copolymers. When fine-tuning, each reasonable molecule will be recorded for the convenience of final analysis and evaluation.

Network Architectures. The implementation of scaffold-decorator network is totally an encoder-decoder architectures with attention mechanism. The encoder is a bidirectional RNN sequenced with an embedding layer and three layers of bidirectional GRU cells of 256 dimensions. Then the hidden states are sent to the decoder, which is a single direction RNN sequenced with an embedding layer, three layers of GRU cells of 256 dimensions. Finally, an global attention layer is adopted to sum up the output of the encoder and the decoder, and a liner layer is connected to calculate the probability of each possible token x_i. The model is trained to maximized the Negative Log-Likehood (NLL) loss, which can be written as:

$$\mathrm{NLL}(\mathbf{S}) = -\sum_{i=1}^{n} logP(x_i|x_{<i}, \mathbf{scaffold}), \tag{8}$$

where $P(x_i|x_{<i})$ is the probability when sampling the $i_t h$ token of decoration sequence **S** with given the previous tokens and the input scaffold. More training protocols and the vocabulary set are supported in supplementary materials.

In previous work [37], molecules in ChEMBL dataset [46] are selected to be sliced into fragment-like decorations using synthetic chemistry constrains (RECAP rules) [47]. Following the work, We also tried to pretrain a scaffold-decorator on ChEMBL dataset, however, since the diversity of the molecules in ChEMBL, the final sampled molecules show complex structures (e.g., double ring nesting) which are out of drug-likeness and hard to be polymerized recognized by

our pharmacologist. Parts of the generated molecules have been shown in supplementary materials. Moreover, the RL agent needs a long time to explore for the desirable area with desirable properties in chemical space. Hence, to solve the above problems, we prepare a new dataset for pretraining, thus the agent can be quickly localized to desirable area.

Data preparation and Knowledge distillation. We collect 29 molecules with ideal structures, including 11 cationic/hydrophobic copolymer monomers and 18 amino acids excluding two of them with the elemental sulphur. In antimicrobial peptide-mimetic copolymers, both the cationic/hydrophobic copolymer monomers are introduced to mimic the amino acid residues. In this way, both of them are chosen helping to find more hidden residue structures.

Then, we adopt a knowledge distillation method with distilling molecules generated from learned grammar rules, thus the explorable chemical space can be greatly shrank than using ChEMBL dataset for more micromesh exploration. In particular, we use a data-efficient graph grammar learning method (DEG) [48] to construct various graph grammar rules from the collected molecules. The dominance of DEG is that all the production rules are learned automatically from the training data, and specific rules can be learned according to the given data.

By applying DEG, we generate additional thousands of molecules which may be close in chemical space and we similarly use the RECAP rules to slice molecules, gaining 1 million pairs of scaffold-decoration data. We use these data to train a distill model with the same structures above and construct a less-focused chemical space for further exploration. (The difference of chemical space can be seen in supplementary information). The distilled model will be fine-tuned with reinforcement learning for customized generation.

Reinforcement Learning. To further guide our distilled model toward relevant areas in chemical space according to customized requirements, we use reinforcement learning for fine-tuning to carry out a constellation of specific tasks. By fine-tuning, various user-defined requirements can be satisfied to generate molecules of interest. In our case, we realized the following requirements: 1) specific fragment structure adjustment of cationic/hydrophobic monomer; 2) monomer generation under various scaffold structures (e.g. "NC([*])CC=O", "NCC(C=O)1[*]C1", 'NC1[*]C1C=O"); 3) multi-objective constrains (e.g. carbon numbers, ring number, HC10/ MIC of S.aureus/MIC of E.coli thresholds). More details will be explained in the following section.

We adopt the REINVENT 2.0 [49] as the RL algorithm and the main roles include a prior model $M_{\textbf{Prior}}$, an agent model $M_{\textbf{Agent}}$ and a score modulating block. The prior model is the distilled decorator generative mdoel introduced above, while the agent model shares the identical network structures and the initialization parameters of the agent model is the completely the same as the prior model. The score modulating block can be seen as the environment which feed back rewards according to the targeted scoring functions.

Then we introduce the reinforcement learning cycle. First, the agent model $M_{\textbf{agent}}$ samples batch of SMILES decorations for a specific scaffold, and the decorated copolymer will be scored according to the scoring function as $S_{\textbf{score}}$ (introduced in the next section). Among each course of sampling molecules, the agent choose the next possible token, seen as the action A, according to the current token sequence, seen as the state S in RL framework. Thus, the agent learn a conditional probability $p(A|S)$ to generate the desired molecules when the episodes go on. To train the agent model, we use the NLL, similar to eq.(8), to represent the agent likelihood of the generated decoration sequence $\mathbf{S}$ as $\mathrm{NLL}(\mathbf{S})_{\textbf{Agent}}$. Then $\mathbf{S}$ will be given to the prior model $M_{\textbf{Prior}}$ to calculate the augmented likelihood with the score $S_{\textbf{score}}(\mathbf{S})$. Ultimately, the loss of the agent can be calculated as:

$$\mathrm{NLL}(\mathbf{S})_{\textbf{Augmented}} = \mathrm{NLL}(\mathbf{S})_{\textbf{Prior}} - \sigma S_{\textbf{score}}(\mathbf{S}) \tag{9}$$

$$\mathrm{loss} = [\mathrm{NLL}(\mathbf{S})_{\textbf{Augmented}} - \mathrm{NLL}(\mathbf{S})_{\textbf{Agent}}]^2, \tag{10}$$

where σ is the scalar value to scale up the output of the score function. During the training process, we collect all valid generated molecules for data analysis, and molecules wit desired properties will be further filtered for experimental validation.

Score and Metric. In this work, we aim to find more potential cationic/hydrophobic monomers combination with specific component ration, which satisfies the desired properties: S.aureus<25, E.coli<25 and HC10>100. Moreover, we design several penalty rules or customized constrains to accelerate the learning process with narrowing down the scope of exploration. The final score function $S_{\textbf{score}}(\mathbf{S})$, which can also be seen as the reward in RL, can be written as:

$$S_{\textbf{score}}(\mathbf{S}) = A*S_{\textbf{property}}(\mathbf{S})+B*S_{\textbf{penalty}}(\mathbf{S})+C*S_{\textbf{constrain}}.(\mathbf{S}), \tag{11}$$

where A, B and C are adjustable weights.

Property score. We use the previously trained predictive network to calculate the values of S.aureus, E.coli and HC10 respectively. For all the calculated values, we apply score transformations (sigmoid for HC10 and revrse sigmoid for MIC of S,aureus and E.coli) so that each component returns a value between [0,1] (the higher the better). This operation helps to avoid one-sided impacts of single-properties and adjust the influence of multiparamerter objectives, and the property scoring function can be written as:

$$S_{\textbf{property}}(\mathbf{S}) = a*\mathrm{MIC}_{\textbf{S.aureus}}(\mathbf{S})+b*\mathrm{MIC}_{\textbf{E.coli}}(\mathbf{S})+c*\mathrm{HC10}(\mathbf{S}), \tag{12}$$

where a, b and c are adjustable weights showing that which the agent should put more focus on.

Penalty score. According to the experience summarized through existing literature, including the suggested elements constrain, carbon number and so on, we design several penalties and constrains to more comprehensively explore the chemical space. To improve the rationality and correctness of the generated molecules, we design several structural penalties as the penalty scoring function,

$$S_{\textbf{penalty}}(\mathbf{S}) = \begin{cases} -5, \text{ when molecule is wrong,} \\ -3, \text{ when unexpected elements exist,} \end{cases} \tag{13}$$

*Constrain score.*To further constrain the structures of the generated molecules, we also design several constrains which can be used alternatively,

$$S_{\textbf{constrain}}(\mathbf{S}) = \begin{cases} C/2, & C \leq 11, \\ -2, & C > 11, \\ N * 0.5, & N > 1, \\ -3 & R > 1, , \end{cases} \tag{14}$$

where C is the carbon number of the final decorated molecule, while N is the number of the atoms which have more than two neighbour atom nodes and R is the ring number.

Metrics. We also introduce two metrics to evaluate and filter the final generated results helping to improve the possibility of being a drug for the candidate copolymer.

Firstly, we introduce the selection index (SI) between the calculated MIC of S.aureus and E.coli, and the value of HC10, which can be calculated as:

$$\mathbf{SI}_{\textbf{S.aureus}} = \mathrm{HC10}/\mathrm{MIC}_{\textbf{S.aureus}}, \mathbf{SI}_{\textbf{E.coli}} = \mathrm{HC10}/\mathrm{MIC}_{\textbf{E.coli}}, \tag{15}$$

The higher the SI is, the better potential the copolymer has to be a drug. Ideal SI for both $\mathbf{SI}_{\textbf{S.aureus}}$ and $\mathbf{SI}_{\textbf{E.coli}}$ is larger than 10.

Secondly, we choose three complementary drug-likeness rules, including Linpinski Rule (ME$\leq$500, logP$\leq$5, Hacc$\leq$10, Hdon$\leq$5) [50], Pfizer Rule (logP$>$3, TPSA$<$75) [51] and GSK rule (200$\leq$MW$\leq$50, -2$\leq$logD$\leq$5) [52]. These rules are derived from the long-standing drug discovery practices of the world's leading pharmaceutical companies. Generated monomers which pass these rules would be filtered out for further consideration.

Evaluation settings We design 11 scaffolds according to the available data and expert recommendations, and the specific structures can be found in supplementary information. To exactly find new candidate copolymers with desired properties and testify the performance of molecular exploration, we set three situations to evaluate the quality of the models. It is worth noting that in all situations, based on the considerations on raw materials, polymerisation difficulty and the synthetic routes design, we fix the cationic monomer and focus on designing new hydrophobic monomers. This helps to improve the synthetic possibility for final validation. Even new cationic monomers are not taken into consideration, it is still a challenging problem since exist multi constrains, involving structures, properties etc. should be taken into consideration. Details are outlined below:

Task 1: Cationic: DM/MM series, hydrophobic: any scaffold, reward design:

$$\begin{aligned} S_{\textbf{score}}(\mathbf{S}) =& 3 * \mathrm{MIC}_{\textbf{S.aureus}}(\mathbf{S}) + 1 * \mathrm{MIC}_{\textbf{E.coli}}(\mathbf{S}) \\ &+ 1 * \mathrm{HC10}(\mathbf{S}) + S_{\textbf{penalty}}(\mathbf{S}). \end{aligned} \tag{16}$$

Task 2: Cationic: DM/MM series, hydrophobic: any scaffold, reward design:

$$\begin{aligned} S_{\textbf{score}}(\mathbf{S}) =& 3 * \mathrm{MIC}_{\textbf{S.aureus}}(\mathbf{S}) + 1 * \mathrm{MIC}_{\textbf{E.coli}}(\mathbf{S}) \\ &+ 1 * \mathrm{HC10}(\mathbf{S}) + S_{\textbf{penalty}}(\mathbf{S}) + S_{\textbf{constrain}}(\mathbf{S}). \end{aligned} \tag{17}$$

Task 3: Cationic: DM series, hydrophobic: NC([*])C C(=O), reward design:

$$\begin{aligned} S_{\textbf{score}}(\mathbf{S}) =& 3 * \mathrm{MIC}_{\textbf{S.aureus}}(\mathbf{S}) + 1 * \mathrm{MIC}_{\textbf{E.coli}}(\mathbf{S}) \\ &+ 1 * \mathrm{HC10}(\mathbf{S}) + S_{\textbf{penalty}}(\mathbf{S}) + S_{\textbf{constrain}}(\mathbf{S}). \end{aligned} \tag{18}$$

We further emphasise that the main purpose of this work is to find candidate cationic-hydrophobic copolymers which can be used as antimicrobial, instead of focusing on testify the novelty or diversity of the molecules generated by the model. Thus, compared with Task 1 and Task 2, we make further qualifications on specific scaffold structure aiming exploring all possible outcomes. All generated molecules whose reward are positive will be recorded for further data analysis helping to find the potential design rules or trends for future design.

REFERENCES

[1] J. H. Kwon and W. G. Powderly, "The post-antibiotic era is here," *Science*, vol. 373, no. 6554, pp. 471–471, 2021.

[2] S. Lu, L. Hu, H. Lin, A. Judge, P. Rivera, M. Palaniappan, B. Sankaran, J. Wang, B. Prasad, and T. Palzkill, "An active site loop toggles between conformations to control antibiotic hydrolysis and inhibition potency for ctx-m β-lactamase drug-resistance enzymes," *Nature Communications*, vol. 13, no. 1, pp. 1–13, 2022.

[3] S. Sharma, P. Barman, S. Joshi, S. Preet, and A. Saini, "Multidrug resistance crisis during covid-19 pandemic: Role of anti-microbial peptides as next-generation therapeutics," *Colloids and Surfaces B: Biointerfaces*, p. 112303, 2021.

[4] J. Tan, J. Tay, J. Hedrick, and Y. Y. Yang, "Synthetic macromolecules as therapeutics that overcome resistance in cancer and microbial infection," *Biomaterials*, vol. 252, p. 120078, 2020.

[5] Z. Xinyu and Z. Chuncai, "Design, synthesis and applications of antimicrobial peptides and antimicrobial peptide-mimetic copolymers," *Progress in Chemistry*, vol. 30, no. 7, p. 913, 2018.

[6] J. Wang, C.-Y. Hsieh, M. Wang, X. Wang, Z. Wu, D. Jiang, B. Liao, X. Zhang, B. Yang, Q. He *et al.*, "Multi-constraint molecular generation based on conditional transformer, knowledge distillation and reinforcement learning," *Nature Machine Intelligence*, vol. 3, no. 10, pp. 914–922, 2021.

[7] J. Jumper, R. Evans, A. Pritzel, T. Green, M. Figurnov, O. Ronneberger, K. Tunyasuvunakool, R. Bates, A. Žídek, A. Potapenko *et al.*, "Highly accurate protein structure prediction with alphafold," *Nature*, vol. 596, no. 7873, pp. 583–589, 2021.

[8] S. Chen and Y. Jung, "A generalized-template-based graph neural network for accurate organic reactivity prediction," *Nature Machine Intelligence*, vol. 4, no. 9, pp. 772–780, 2022.

[9] S. Chawla, A. Rockstroh, M. Lehman, E. Ratther, A. Jain, A. Anand, A. Gupta, N. Bhattacharya, S. Poonia, P. Rai *et al.*, "Gene expression based inference of cancer drug sensitivity," *Nature communications*, vol. 13, no. 1, pp. 1–15, 2022.

[10] F. X. Galdos, S. Xu, W. R. Goodyer, L. Duan, Y. V. Huang, S. Lee, H. Zhu, C. Lee, N. Wei, D. Lee *et al.*, "devcellpy is a machine learning-enabled pipeline for automated annotation of complex multilayered single-cell transcriptomic data," *Nature communications*, vol. 13, no. 1, pp. 1–20, 2022.

[11] A. Zhavoronkov, Y. A. Ivanenkov, A. Aliper, M. S. Veselov, V. A. Aladinskiy, A. V. Aladinskaya, V. A. Terentiev, D. A. Polykovskiy, M. D. Kuznetsov, A. Asadulaev *et al.*, "Deep learning enables rapid identification of potent ddr1 kinase inhibitors," *Nature biotechnology*, vol. 37, no. 9, pp. 1038–1040, 2019.

[12] P. Das, T. Sercu, K. Wadhawan, I. Padhi, S. Gehrmann, F. Cipcigan, V. Chenthamarakshan, H. Strobelt, C. Dos Santos, P.-Y. Chen *et al.*, "Accelerated antimicrobial discovery via deep generative models and molecular dynamics simulations," *Nature Biomedical Engineering*, vol. 5, no. 6, pp. 613–623, 2021.

[13] S. Zheng, Y. Tan, Z. Wang, C. Li, Z. Zhang, X. Sang, H. Chen, and Y. Yang, "Accelerated rational protac design via deep learning and molecular simulations," *Nature Machine Intelligence*, vol. 4, no. 9, pp. 739–748, 2022.

[14] D. Veltri, U. Kamath, and A. Shehu, "Deep learning improves antimicrobial peptide recognition," *Bioinformatics*, vol. 34, no. 16, pp. 2740–2747, 2018.

[15] Y. Ma, Z. Guo, B. Xia, Y. Zhang, X. Liu, Y. Yu, N. Tang, X. Tong, M. Wang, X. Ye *et al.*, "Identification of antimicrobial peptides from the human gut microbiome using deep learning," *Nature Biotechnology*, pp. 1–11, 2022.

[16] N. W. Gebauer, M. Gastegger, S. S. Hessmann, K.-R. Müller, and K. T. Schütt, "Inverse design of 3d molecular structures with conditional generative neural networks," *Nature communications*, vol. 13, no. 1, pp. 1–11, 2022.

[17] P. G. Polishchuk, T. I. Madzhidov, and A. Varnek, "Estimation of the size of drug-like chemical space based on gdb-17 data," *Journal of computer-aided molecular design*, vol. 27, no. 8, pp. 675–679, 2013.

[18] L. Tao, J. Byrnes, V. Varshney, and Y. Li, "Machine learning strategies for the structure-property relationship of copolymers," *Available at SSRN 4071024*, 2022.

[19] K. Hanaoka, "Deep neural networks for multicomponent molecular systems," *ACS omega*, vol. 5, no. 33, pp. 21 042–21 053, 2020.

[20] C. Kuenneth, W. Schertzer, and R. Ramprasad, "Copolymer informatics with multitask deep neural networks," *Macromolecules*, vol. 54, no. 13, pp. 5957–5961, 2021.

[21] Z. Guo, W. Yu, C. Zhang, M. Jiang, and N. V. Chawla, "Graseq: graph and sequence fusion learning for molecular property prediction," in *Proceedings of the 29th ACM International Conference on Information & Knowledge Management*, 2020, pp. 435–443.

[22] A. Paul, D. Jha, R. Al-Bahrani, W.-k. Liao, A. Choudhary, and A. Agrawal, "Chemixnet: Mixed dnn architectures for predicting chemical properties using multiple molecular representations," in *NIPS*, 2018.

[23] G. A. Pinheiro, J. L. Da Silva, and M. G. Quiles, "Smiclr: Contrastive learning on multiple molecular representations for semisupervised and unsupervised representation learning," *Journal of Chemical Information and Modeling*, vol. 62, no. 17, pp. 3948–3960, 2022.

[24] A. Tiihonen, S. J. Cox-Vazquez, Q. Liang, M. Ragab, Z. Ren, N. T. P. Hartono, Z. Liu, S. Sun, C. Zhou, N. C. Incandela *et al.*, "Predicting antimicrobial activity of conjugated oligoelectrolyte molecules via machine learning," *Journal of the American Chemical Society*, vol. 143, no. 45, pp. 18 917–18 931, 2021.

[25] T.-S. Lin, C. W. Coley, H. Mochigase, H. K. Beech, W. Wang, Z. Wang, E. Woods, S. L. Craig, J. A. Johnson, J. A. Kalow *et al.*, "Bigsmiles: a structurally-based line notation for describing macromolecules," *ACS central science*, vol. 5, no. 9, pp. 1523–1531, 2019.

[26] Q. Zhang, P. Ma, J. Xie, S. Zhang, X. Xiao, Z. Qiao, N. Shao, M. Zhou, W. Zhang, C. Dai *et al.*, "Host defense peptide mimicking poly-β-peptides with fast, potent and broad spectrum antibacterial activities," *Biomaterials science*, vol. 7, no. 5, pp. 2144–2151, 2019.

[27] B. P. Mowery, S. E. Lee, D. A. Kissounko, R. F. Epand, R. M. Epand, B. Weisblum, S. S. Stahl, and S. H. Gellman, "Mimicry of antimicrobial host-defense peptides by random copolymers," *Journal of the American Chemical Society*, vol. 129, no. 50, pp. 15 474–15 476, 2007.

[28] J. Zhang, D. A. Kissounko, S. E. Lee, S. H. Gellman, and S. S. Stahl, "Access to poly-β-peptides with functionalized side chains and end groups via controlled ring-opening polymerization of β-lactams," *Journal of the American Chemical Society*, vol. 131, no. 4, pp. 1589–1597, 2009.

[29] D. Zhang, Q. Chen, W. Zhang, H. Liu, J. Wan, Y. Qian, B. Li, S. Tang, Y. Liu, S. Chen *et al.*, "Silk-inspired β-peptide materials resist fouling and the foreign-body response," *Angewandte Chemie*, vol. 132, no. 24, pp. 9673–9680, 2020.

[30] H. Moriwaki, Y.-S. Tian, N. Kawashita, and T. Takagi, "Mordred: a molecular descriptor calculator," *Journal of cheminformatics*, vol. 10, no. 1, pp. 1–14, 2018.

[31] S. Zheng, X. Yan, Y. Yang, and J. Xu, "Identifying structure–property relationships through smiles syntax analysis with self-attention mechanism," *Journal of chemical information and modeling*, vol. 59, no. 2, pp. 914–923, 2019.

[32] Y. Song, S. Zheng, Z. Niu, Z.-H. Fu, Y. Lu, and Y. Yang, "Communicative representation learning on attributed molecular graphs," in *Proceedings of the Twenty-Ninth International Conference on International Joint Conferences on Artificial Intelligence*, 2021, pp. 2831–2838.

[33] A. Vaswani, N. Shazeer, N. Parmar, J. Uszkoreit, L. Jones, A. N. Gomez, Ł. Kaiser, and I. Polosukhin, "Attention is all you need," *Advances in neural information processing systems*, vol. 30, 2017.

[34] C. Ying, T. Cai, S. Luo, S. Zheng, G. Ke, D. He, Y. Shen, and T.-Y. Liu, "Do transformers really perform badly for graph representation?" *Advances in Neural Information Processing Systems*, vol. 34, pp. 28 877–28 888, 2021.

[35] S. S. SV, J. Law, C. Tripp, D. Duplyakin, E. Skordilis, D. Biagioni, R. Paton, and P. S. John, "Multi-objective goal-directed optimization of de novo stable organic radicals for aqueous redox flow batteries," *Nature Machine Intelligence*, vol. 4, no. 8, pp. 720–730, 2022.

[36] Y. Li, L. Zhang, Y. Wang, J. Zou, R. Yang, X. Luo, C. Wu, W. Yang, C. Tian, H. Xu *et al.*, "Generative deep learning enables the discovery of a potent and selective ripk1 inhibitor," *Nature Communications*, vol. 13, no. 1, pp. 1–18, 2022.

[37] J. Arús-Pous, A. Patronov, E. J. Bjerrum, C. Tyrchan, J.-L. Reymond, H. Chen, and O. Engkvist, "Smiles-based deep generative scaffold decorator for de-novo drug design," *Journal of cheminformatics*, vol. 12, no. 1, pp. 1–18, 2020.

[38] L. McInnes, J. Healy, N. Saul, and L. Großberger, "Umap: Uniform manifold approximation and projection," *Journal of Open Source Software*, vol. 3, no. 29, 2018.

[39] Q. Ren, Q. Chen, L. Ren, C. Cao, R. Liu, and Y. Cheng, "Amphipathic poly-β-peptides for intracellular protein delivery," *Chemical Communications*, vol. 58, no. 27, pp. 4320–4323, 2022.

[40] P. Ma, Y. Wu, W. Jiang, N. Shao, M. Zhou, Y. Chen, J. Xie, Z. Qiao, and R. Liu, "Biodegradable peptide polymers as alternatives to antibiotics used in aquaculture," *Biomaterials Science*, 2022.

[41] J. Zou, M. Zhou, Z. Ji, X. Xiao, Y. Wu, R. Cui, S. Deng, and R. Liu, "Controlled copolymerization of α-ncas and α-nntas for preparing peptide/peptoid hybrid polymers with adjustable proteolysis," *Polymer Chemistry*, vol. 13, no. 3, pp. 388–394, 2022.

[42] Q. Chen, D. Zhang, W. Zhang, H. Zhang, J. Zou, M. Chen, J. Li, Y. Yuan, and R. Liu, "Dual mechanism β-amino acid polymers promoting cell adhesion," *Nature communications*, vol. 12, no. 1, pp. 1–13, 2021.

[43] Y. Wu, D. Zhang, P. Ma, R. Zhou, L. Hua, and R. Liu, "Lithium hexamethyldisilazide initiated superfast ring opening polymerization of alpha-amino acid n-carboxyanhydrides," *Nature communications*, vol. 9, no. 1, pp. 1–10, 2018.

[44] R. A. Patel, C. H. Borca, and M. A. Webb, "Featurization strategies for polymer sequence or composition design by machine learning," *Molecular Systems Design & Engineering*, 2022.

[45] I. Guyon, J. Weston, S. Barnhill, and V. Vapnik, "Gene selection for cancer classification using support vector machines," *Machine learning*, vol. 46, no. 1, pp. 389–422, 2002.

[46] A. Gaulton, A. Hersey, M. Nowotka, A. P. Bento, J. Chambers, D. Mendez, P. Mutowo, F. Atkinson, L. J. Bellis, E. Cibrián-Uhalte *et al.*, "The chembl database in 2017," *Nucleic acids research*, vol. 45, no. D1, pp. D945–D954, 2017.

[47] X. Q. Lewell, D. B. Judd, S. P. Watson, and M. M. Hann, "Recap retrosynthetic combinatorial analysis procedure: a powerful new technique for identifying privileged molecular fragments with useful applications in combinatorial chemistry," *Journal of chemical information and computer sciences*, vol. 38, no. 3, pp. 511–522, 1998.

[48] M. Guo, V. Thost, B. Li, P. Das, J. Chen, and W. Matusik, "Data-efficient graph grammar learning for molecular generation," in *International Conference on Learning Representations*, 2021.

[49] T. Blaschke, J. Arús-Pous, H. Chen, C. Margreitter, C. Tyrchan, O. Engkvist, K. Papadopoulos, and A. Patronov, "Reinvent 2.0: an ai tool for de novo drug design," *Journal of chemical information and modeling*, vol. 60, no. 12, pp. 5918–5922, 2020.

[50] C. A. Lipinski, F. Lombardo, B. W. Dominy, and P. J. Feeney, "Experimental and computational approaches to estimate solubility and permeability in drug discovery and development settings," *Advanced drug delivery reviews*, vol. 23, no. 1-3, pp. 3–25, 1997.

[51] J. D. Hughes, J. Blagg, D. A. Price, S. Bailey, G. A. DeCrescenzo, R. V. Devraj, E. Ellsworth, Y. M. Fobian, M. E. Gibbs, R. W. Gilles *et al.*, "Physiochemical drug properties associated with in vivo toxicological outcomes," *Bioorganic & medicinal chemistry letters*, vol. 18, no. 17, pp. 4872–4875, 2008.

[52] M. P. Gleeson, "Generation of a set of simple, interpretable admet rules of thumb," *Journal of medicinal chemistry*, vol. 51, no. 4, pp. 817–834, 2008.